INORGANIC CHEMISTRY FRONTIERS

RESEARCH ARTICLE

View Article Online
View Journal | View Issue

Cite this: *Inorg. Chem. Front.*, 2022, **9**, 1812

A highly stable Zn_9-pyrazolate metal–organic framework with metallosalen ligands as a carbon dioxide cycloaddition catalyst†

Fa-Xue Ma,[a,b] Fu-Qi Mi,[b] Meng-Jiao Sun,[b,c] Tao Huang,[b] Zi-An Wang,[b] Teng Zhang *[b,c] and Rong Cao *[a,b,c]

Received 14th December 2021,
Accepted 13th January 2022

DOI: 10.1039/d1qi01555a

rsc.li/frontiers-inorganic

A three-dimensional (3D) metal–organic framework constructed from unprecedented $Zn_9O_2(OH)_2(pyz)_{12}$ (pyz = pyrazolate) clusters and Ni(salen)-derived linkers was reported. The MOF exhibits high catalytic activity for CO_2 cycloaddition reactions with excellent stability. The MOF catalyst can be recycled at least 15 times without loss of activity and the turnover number (TON) per Ni site can reach as high as 2887.

As emerging materials, porous metal–organic frameworks (MOFs) have attracted much attention for applications in gas storage and separation,[1] chemical sensing,[2,3] catalysis,[4] and many other fields over the past two decades.[5] MOFs are constructed from organic linkers, usually polycarboxylates[6,7] or polyazolates,[8,9] and metal/metal cluster nodes, and thus are of rich structural and functional diversity that allows their fine-tuning and modification to meet different requirements of the mentioned applications. However, challenges remain. Chemical stability is one of the major concerns for further applications of MOFs.[10–12] Several strategies have been developed to design more stable MOFs: (i) increasing the metal–ligand interaction strength with high pK_a ligands (*e.g.* azoles) and/or high-valent metal ions (*e.g.* Zr^{4+},Cr^{3+});[13,14] (ii) reducing the contact between water or aqueous attacking reagents and the coordination bonds of host frameworks;[15] (iii) increasing the rigidity of ligands to enhance the stability.[16] MOFs based on azolate donors usually show better stability than those of carboxylate donors because the sp^2 N atoms tend to adopt saturated coordination and thus become locally hydrophobic and unavailable for interaction with attacking reagents.[17,18] Meanwhile, interpenetrated motifs also significantly enhance the framework stability.[19] It is not only because interpenetrated networks could reduce the pore size and increase the wall thickness, but also due to the higher strength of non-covalent interactions in interpenetrated structures which lock the linkers in place and prevent their displacement.[15]

Metallosalen complexes are one of the earliest developed and most widely explored categories of asymmetric transition metal catalysts.[20–22] Since the early 1990s, metallosalen complexes have found catalytic applications for olefin epoxidation,[23] aldehyde cyanation,[24] epoxide ring-opening[25] and CO_2 cycloaddition reactions.[26,27] Heterogenized metallosalen catalysts have been constructed as surface-grafted silica or resins,[28] MOFs,[29–31] covalent organic frameworks (COFs),[32,33] and porous organic polymers (POPs)[34] for better catalyst separation and recyclability. However, it is still challenging to balance the catalytic activity/selectivity with material stability. MOF catalysts based on metallosalen-derived polycarboxylate linkers have shown exceptional catalytic performance compared to other heterogeneous metallosalen catalysts,[35–38] but the stability of those materials is not yet satisfactory.[17]

Herein, we report the synthesis and catalytic applications of a zinc-pyrazolate MOF constructed from Ni(salen) bispyrazolate ligands and unprecedented Zn_9 clusters. The zinc-pyrazolate connection allows the MOF to withstand acid and base treatments as well as boiling water. The MOF also exhibits high catalytic activity and exceptional recyclability for CO_2-epoxide cycloaddition reactions.

The Zn_9-pyrazolate MOF $Zn_9O_2(OH)_2(L)_6$ was obtained by a solvothermal reaction between $Zn(OAc)_2{\cdot}6H_2O$ and the Ni(salen)-derived ligand H_2L (Fig. 1b and Scheme S1†) in a DMF/H_2O/trifluoroacetic acid mixture solution. As shown in the scanning electron microscopy (SEM) image, the crystalline MOF particles are of oblique dodecahedron shape with a uniform size of 20 μm (Fig. 1d). The exact formula and structure of the MOF were determined by single-crystal X-ray diffraction (SCXRD) studies. Preliminary reflection data reduction

[a]*College of Chemistry and Chemical Engineering, Xiamen University, Xiamen 361005, China. E-mail: rcao@fjirsm.ac.cn*
[b]*State Key Laboratory of Structural Chemistry, Fujian Institute of Research on the Structure of Matter, Chinese Academy of Sciences, Fuzhou 350002, China. E-mail: zhangteng@fjirsm.ac.cn*
[c]*University of the Chinese Academy of Sciences, Beijing 100049, China*

†Electronic supplementary information (ESI) available.CCDC 2128369. For ESI and crystallographic data in CIF or other electronic format see DOI: 10.1039/d1qi01555a

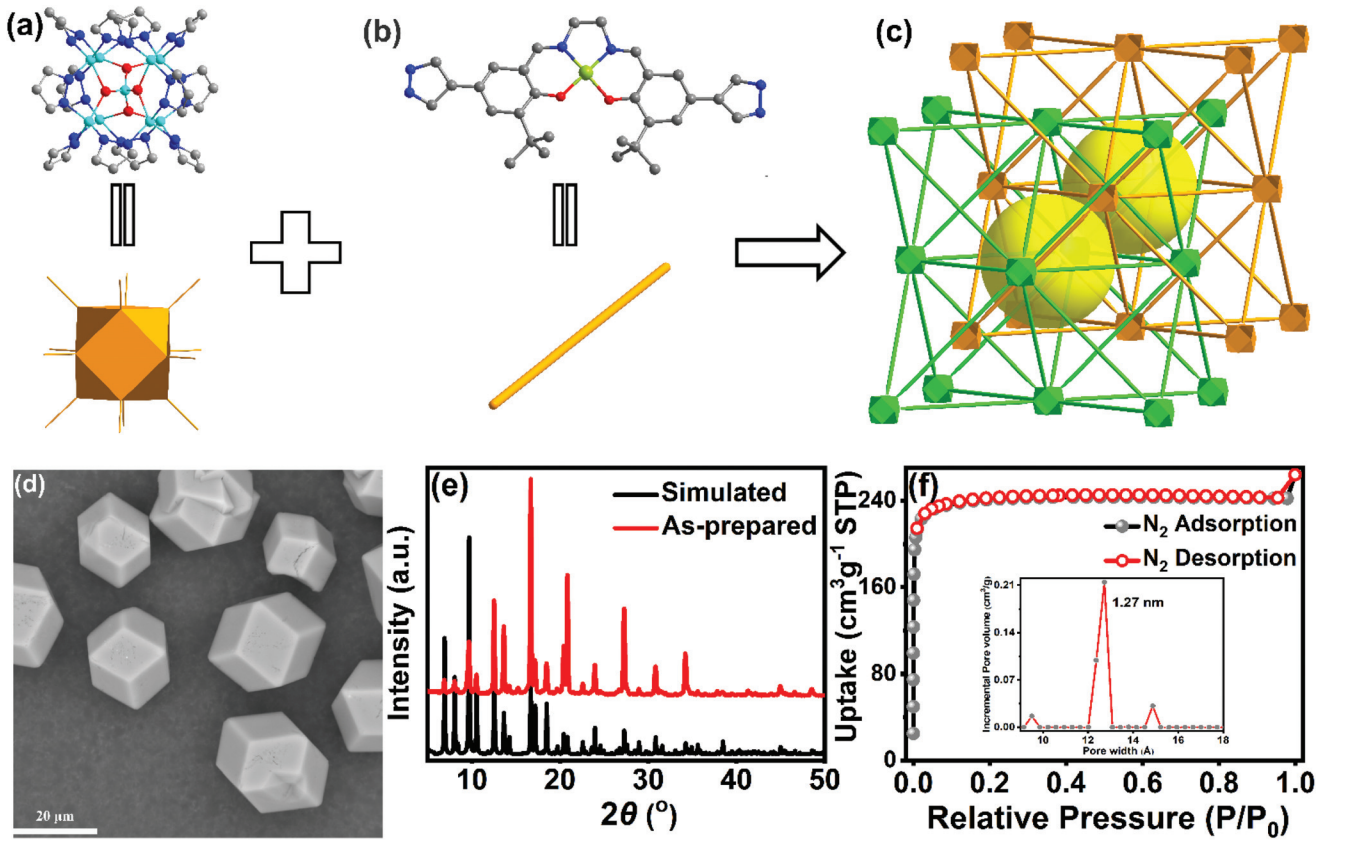

Fig. 1 Construction of the $Zn_9O_2(OH)_2(L)_6$ MOF (Zn: turquoise; Ni: lime; N: blue; O: red.): (a) the $Zn_9O_2(OH)_2(pyrazolate)_{12}$ node; (b) the Ni(salen)-derived bis(pyrazolate) ligand; (c) two-fold interpenetration structure of the $Zn_9O_2(OH)_2(L)_6$ MOF; (d) SEM image of $Zn_9O_2(OH)_2(L)_6$; (e) simulated and experimental PXRD patterns of $Zn_9O_2(OH)_2(L)_6$; (f) N_2 sorption isotherms of the $Zn_9O_2(OH)_2(L)_6$ MOF (inset: pore size distribution by the NLDFT method).

indicates that the MOF crystallizes in the cubic $Fd\bar{3}m$ space group. Further structure refinement revealed that the L^{2-} linker exhibits symmetry-related, two-fold disorder. To better describe the structure, the apparent symmetry of the framework was arbitrarily lowered to the chiral $F4_132$ space group with a racemic twinning parameter accounting for the disorder. The MOF has a formula of $Zn_9O_2(OH)_2(L)_6$ and contains an unprecedented $[Zn_9O_2(OH)_2(pyz)_{12}]$ cluster secondary building unit (SBU) (Fig. 1a). In the SBU, eight Zn atoms are located at the eight vertexes of a cuboid with an additional Zn atom at the center. The central Zn(II) atom adopts a distorted tetrahedral ZnO_4 coordination sphere, while the four O atoms connect to eight vertical Zn(II) atoms in a μ_3-O fashion (Fig. 1a). The twelve pyrazolate groups coordinate to the Zn_9 cuboid cluster from the directions of twelve edges; therefore, each vertical Zn(II) ion is tetracoordinated in a ZnN_3O fashion. The Zn–Zn distances between vertical and central Zn(II) ions are 3.06 Å and 3.14 Å, respectively, and the distances between vertical Zn(II) ions are 3.58 Å, showing no intermetallic bonding. Previous studies on zinc-pyrazolate coordination chemistry have found $[Zn_4O(pyz)_6]$ and $[Zn_3O(pyz)_3]$ clusters, and ZnN_4 tetrahedron SBUs;[18,39–41] yet to the best of our knowledge, the $[Zn_9O_2(OH)_2(pyz)_{12}]$ cluster has never been reported. The $Zn_9O_2(OH)_2$ cluster SBU is connected to twelve adjacent SBUs through Ni(salen)-based bis(pyrazolate) linkers to form a 3D network with face-centered cubic unit (**fcu**) topology, the same as that constructed from Ni_8 clusters and linear bis(pyrazolate) linkers.[42] The MOF adopts a two-fold interpenetration structure, which is unprecedented in previous Ni_8(pyrazolate) MOFs.[42–45] The Zn_9 cluster of one network is located in the tetrahedral cavity formed by another network with 50% occupancy (Fig.S4†). The two interpenetrating networks are symmetrically related by the 4_1 screw axis and pseudo *d* glide plane. Because of the interpenetration, the pore size of the $Zn_9O_2(OH)_2(L)_6$MOF is only 10 Å as measured from the single crystal structure, a relatively small value compared to the ligand length. The powder X-ray diffraction (PXRD) pattern of the bulk MOF sample matches well with that from single-crystal structure simulation, confirming the phase purity (Fig. 1e). X-ray photoelectron spectroscopy (XPS) shows that both Zn and Ni are in the +2 oxidation state (Fig. S5†).

The N_2 sorption isotherms (Fig. 1f) of $Zn_9O_2(OH)_2(L)_6$ revealed a typical type I behavior with a Brunauer–Emmett–Teller (BET) surface area of 934 m^2g^{-1}. Non-local density functional theory (NLDFT) pore size distribution analysis gave a

total pore volume of 0.215 cm^3g^{-1} with a pore size of 12.7 Å (Fig. 1f), which is in good agreement with the two-fold interpenetration structure. The CO_2 sorption isotherm (Fig. S7a†) gave a maximum CO_2 uptake of 168 cm^3g^{-1}. The $Zn_9O_2(OH)_2(L)_6$ MOF retained its crystallinity even after sorption tests as shown by the unchanged diffraction peaks (Fig.S7b†).

To explore the chemical stability of $Zn_9O_2(OH)_2(L)_6$, the MOF samples were treated with HCl, NaOH and ammonia aqueous solutions at room temperature, and H_2O and HCl upon heating. In pH 2 HCl, 2.5% ammonia, and 2 M NaOH solutions, the MOF samples were stable for at least 210 days at room temperature as indicated by the PXRD patterns (Fig. 2). In pH 3 HCl and H_2O, the MOF samples were stable for at least 21 days at 100 °C (Fig. 2 and S8†). Therefore, $Zn_9O_2(OH)_2(L)_6$ exhibits better chemical stability compared with most pyrazolate-based MOFs (Table S3†).[46,47] Such good stability could be attributed to a combination of several effects. First, the Zn-pyrazole saturated coordination protects the metal centre from being attacked by a base.[10,48] Second, the two-fold interpenetrated structure reduces the MOF porosity and inhibits guest diffusion through MOF channels, making the MOF more stable.[15,49] Third, the pyrazolate ligand with hydrophobic *t*-butyl group modification results in a hydrophobic MOF with a water contact angle of 114° (Fig. S9†), further reducing the contact of the MOF with aqueous attacking reagents.[42] All these effects taken together lead to the high chemical stability of $Zn_9O_2(OH)_2(L)_6$.

Great interest has been shown in converting CO_2 into value-added chemicals and reducing the greenhouse gas concentration in the atmosphere. The cycloaddition of CO_2 with epoxides (Scheme 1) has been widely proposed as an effective approach for that purpose due to its near-100% atomic efficiency.[50,51] Different types of catalysts, including organocatalysts,[52] ionic liquids,[53] metallosalen complexes,[26] single atom catalysts[54] and other coordination compounds,[55,56] have been reported as effective catalysts for CO_2 cycloaddition reactions. POPs[34] and MOFs[38,57–60] have been reported as the heterogeneous version of those molecular catalysts to facilitate the separation and recycling processes. Given the high stability of the Ni(salen)-derived $Zn_9O_2(OH)_2(L)_6$ MOF, we expected that it could be a good candidate as a heterogeneous CO_2 cycloaddition catalyst. We first investigated its catalytic activity with styrene oxide as a model substrate. The reaction was almost complete in 24 hours at 80 °C in the presence of 1.5% MOF catalyst and 1.5% tetrabutylammonium bromide (TBAB) co-catalyst and under 7 bar CO_2 atmosphere. When the MOF and TBAB loading was decreased from 1.5% to 0.5%, the yield of the carbonate product only decreased from 99% to 95% (entries 1 and 2, Table 1), indicating the high catalytic activity of the MOF/TBAB catalyst. When either the MOF or TBAB was absent, the product yield was much lower under the same pressure and temperature conditions (Fig. 3a and entries 3 and 4, Table 1), showing that both the components are necessary for the catalysis. Using the Ni(salen)-derived ligand H_2L instead of the MOF gave a similar yield for styrene carbonate, showing that the ligand is the catalytically active component (entry 5, Table 1). Reducing the reaction temperature or pressure led to lower yields, yet such an effect can be compensated for by increasing the catalyst loading to 1% (entries 6–8, Table 1).

The high chemical stability of the $Zn_9O_2(OH)_2(L)_6$ MOF allows easy recycling of the catalysts. After the reaction, the MOF catalyst was simply filtered off and washed to remove product residues in the pores, and then it was added to another batch of reactants. In this way, the MOF catalyst can be recycled at least 15 times without any loss in its catalytic activity (Fig. 3b). A total turnover number (TON) of more than 2887 was achieved after 15 cycles. SEM, PXRD and N_2 sorption experiments showed that the MOF maintains the original morphology, structure and porosity after catalysis (Fig.S11†).

The catalytic activity of the $Zn_9O_2(OH)_2(L)_6$ MOF for substrates with different sizes was also investigated. With the increasing molecular sizes of the substrates, the isolated yields

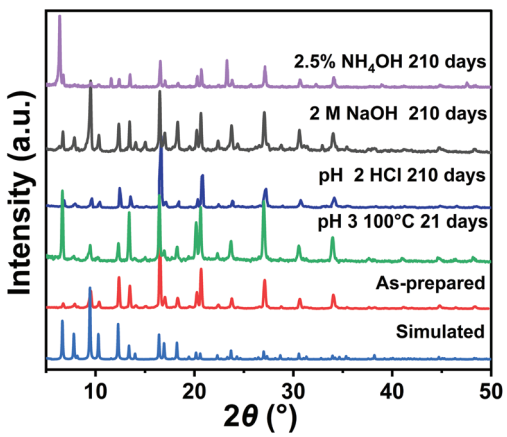

Fig. 2 PXRD patterns of the as-prepared $Zn_9O_2(OH)_2(L)_6$ and those after acid, base and heating treatments.

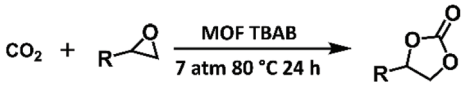

Scheme 1 CO_2 cycloaddition reaction catalyzed by the MOF and TBAB.

Table 1 Optimization of reaction conditions for the cycloaddition of CO_2 with styrene oxide

Entry	Catalyst (%)	TBAB (%)	*P* (atm)	*T* (°C)	Conversion (%)
1	1.5	1.5	7	80	99
2	0.5	0.5	7	80	95
3	0.5	0	7	80	8
4	0	0.5	7	80	34
5[a]	0.5	0.5	7	80	90
6	0.5	0.5	4	80	68
7	0.5	0.5	7	60	67
8	1	1	4	80	95

[a] The ligand H_2L was used instead of the MOF.

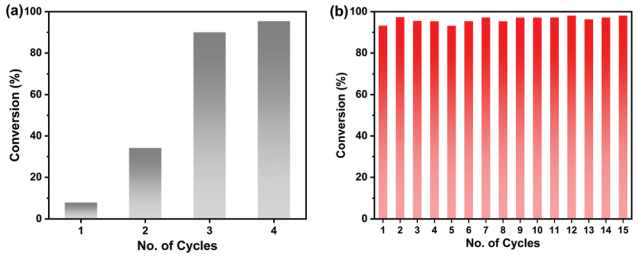

Fig. 3 (a) Styrene oxide conversions with different catalysts; (b) styrene oxide conversions at different runs in the reuse experiments for CO_2 cycloaddition. Reaction conditions: 80 °C, 7 atm CO_2, 0.5% MOF catalyst and 0.5% TBAB co-catalyst.

for the corresponding carbonate products showed a descending trend of 89%, 30%, and 9% for epichlorohydrin, styrene oxide, and stilbene oxide, respectively (Table S4†). The size-dependent conversion, therefore, demonstrates that the catalysis takes place in the MOF channels and not only on the external surface.

We next explored the catalytic activity of the MOF/TBAB system with different epoxide substrates. As shown in Table 2, the MOF/TBAB catalyst showed good conversion for epichlorohydrin (99%), phenyl glycidyl ether (98%) and cyclopentene oxide (82%) substrates, and moderate conversion for cyclohexene oxide (24%). It is worth noting that cyclohexene oxide is one of the very inactive substrates owing to its steric hindrance originating from the bicyclic structure.[61] However, the yield of cyclohexene carbonate can be optimized to 82% by increasing the catalyst loading to 1.5%. This yield outperformed many previously reported heterogeneous catalysts under similar loading, temperature, and pressure conditions (Table S5†). The results fully demonstrate that the MOF has excellent catalytic activity and provides a convincing experimental basis for industrial applications.

In summary, we reported the synthesis of a Zn-pyrazolate MOF with an unprecedented $Zn_9O_2(OH)_2(pyz)_{12}$ cluster and a two-fold interpenetration network structure. This MOF exhibits excellent chemical and stability in pH 2–14 aqueous solutions as well as in boiling water or weak acids. The MOF efficiently catalyzes CO_2 cycloaddition reactions with various epoxide substrates, showing its high activity and exceptional recyclability. Consequently, this work will offer significant guidance in the design and synthesis of highly stable metal–pyrazolate MOFs, thereby promoting the discovery of their structures as well as potential applications.

Table 2 Cycloaddition reactions of CO_2 with different epoxide substrates

Entry	Substrate	Catalyst (%)	TBAB (%)	Conversion (%)	Yield (%)
1		0.5	0.5	99	96
2		0.5	0.5	98	97
3		0.5	0.5	82	78
4		0.5	0.5	24	19
5		1.5	1.5	82	79

Conflicts of interest

The authors declare no conflict of interest.

Acknowledgements

This work is financially supported by the National Key Research and Development Program of China (2017YFA0700103) and the National Natural Science Foundation of China (Grant No. 22005306). The authors greatly thank Prof. Li-Xin Wu (FJIRSM, CAS) for the help with contact angle measurements, Prof. Xin-Qiang Fang (FJIRSM, CAS) for the help with ee determination, and Bai-Tong Liu (FJIRSM, CAS), Jia-Wei Chen (XMU) and Shi-Rui Zhang (SNNU) for the help with crystallography and N_2 sorption analysis.

Notes and references

1 P. Q. Liao, N. Y. Huang, W. X. Zhang, J. P. Zhang and X. M. Chen, Controlling guest conformation for efficient purification of butadiene, *Science*, 2017, **356**, 1193–1196.
2 Y. Cui, B. Li, H. He, W. Zhou, B. Chen and G. Qian, Metal-Organic Frameworks as Platforms for Functional Materials, *Acc. Chem. Res.*, 2016, **49**, 483–493.
3 M. L. Hu, S. A. A. Razavi, M. Piroozzadeh and A. Morsali, Sensing organic analytes by metal-organic frameworks: a new way of considering the topic, *Inorg. Chem. Front.*, 2020, **7**, 1598–1632.
4 Y. B. Huang, J. Liang, X. S. Wang and R. Cao, Multifunctional metal-organic framework catalysts: synergistic catalysis and tandem reactions, *Chem. Soc. Rev.*, 2017, **46**, 126–157.
5 H. Furukawa, K. E. Cordova, M. O'Keeffe and O. M. Yaghi, The chemistry and applications of metal-organic frameworks, *Science*, 2013, **341**, 1230444.
6 Y. Bai, Y. Dou, L. H. Xie, W. Rutledge, J. R. Li and H. C. Zhou, Zr-based metal-organic frameworks: design, synthesis, structure, and applications, *Chem. Soc. Rev.*, 2016, **45**, 2327–2367.
7 W. Gong, Y. Liu, H. Y. Li and Y. Cui, Metal-organic frameworks as solid Brønsted acid catalysts for advanced organic transformations, *Coord. Chem. Rev.*, 2020, **420**, 213400.
8 C. Pettinari, A. Tabacaru and S. Galli, Coordination polymers and metal-organic frameworks based on poly(pyrazole)-containing ligands, *Coord. Chem. Rev.*, 2016, **307**, 1–31.

9 J. P. Zhang, H. L. Zhou, D. D. Zhou, P. Q. Liao and X. M. Chen, Controlling flexibility of metal-organic frameworks, *Natl. Sci. Rev.*, 2018, **5**, 907–919.
10 N. Li, J. Xu, R. Feng, T. L. Hu and X. H. Bu, Governing metal-organic frameworks towards high stability, *Chem. Commun.*, 2016, **52**, 8501–8513.
11 H. He, Q. Sun, W. Gao, J. A. Perman, F. Sun, G. Zhu, B. Aguila, K. Forrest, B. Space and S. Ma, A Stable Metal-Organic Framework Featuring a Local Buffer Environment for Carbon Dioxide Fixation, *Angew. Chem., Int. Ed.*, 2018, **57**, 4657–4662.
12 C. Healy, K. M. Patil, B. H. Wilson, L. Hermanspahn, N. C. Harvey-Reid, B. I. Howard, C. Kleinjan, J. Kolien, F. Payet, S. G. Telfer, P. E. Kruger and T. D. Bennett, The thermal stability of metal-organic frameworks, *Coord. Chem. Rev.*, 2020, **419**, 213388.
13 K. S. Park, Z. Ni, A. P. Côté, J. Y. Choi, R. Huang, F. J. Uribe-Romo, H. K. Chae, M. O'Keeffe and O. M. Yaghi, Exceptional chemical and thermal stability of zeolitic imidazolate frameworks, *Proc. Natl. Acad. Sci. U. S. A.*, 2006, **103**, 10186–10191.
14 G. Huang, L. Yang, Q. Yin, Z. B. Fang, X. J. Hu, A. A. Zhang, J. Jiang, T. F. Liu and R. Cao, A Comparison of Two Isoreticular Metal-Organic Frameworks with Cationic and Neutral Skeletons: Stability, Mechanism, and Catalytic Activity, *Angew. Chem., Int. Ed.*, 2020, **59**, 4385–4390.
15 M. Ding, X. Cai and H. L. Jiang, Improving MOF stability: approaches and applications, *Chem. Sci.*, 2019, **10**, 10209–10230.
16 X. L. Lv, S. Yuan, L. H. Xie, H. F. Darke, Y. Chen, T. He, C. Dong, B. Wang, Y. Z. Zhang, J. R. Li and H. C. Zhou, Ligand Rigidification for Enhancing the Stability of Metal-Organic Frameworks, *J. Am. Chem. Soc.*, 2019, **141**, 10283–10293.
17 A. V. Desai, S. Sharma, S. Let and S. K. Ghosh, N-donor linker based metal-organic frameworks (MOFs): Advancement and prospects as functional materials, *Coord. Chem. Rev.*, 2019, **395**, 146–192.
18 A. A. Zhang, X. Cheng, X. He, W. Liu, S. Deng, R. Cao and T. F. Liu, Harnessing Electrostatic Interactions for Enhanced Conductivity in Metal-Organic Frameworks, *Research*, 2021, **2021**, 9874273.
19 H. L. Jiang, T. A. Makal and H. C. Zhou, Interpenetration control in metal-organic frameworks for functional applications, *Coord. Chem. Rev.*, 2013, **257**, 2232–2249.
20 E. N. Jacobsen, W. Zhang, A. R. Muci, J. R. Ecker and L. Deng, Highly Enantioselective Epoxidation Catalysts Derived from 1,2-Diaminocyclohexane, *J. Am. Chem. Soc.*, 1991, **113**, 7063–7064.
21 E. J. Allain, L. P. Hager, L. Deng and E. N. Jacobsen, Highly Enantioselective Epoxidation of Disubstituted Alkenes with Hydrogen-Peroxide Catalyzed by Chloroperoxidase, *J. Am. Chem. Soc.*, 1993, **115**, 4415–4416.
22 M. Palucki, P. J. Pospisil, W. Zhang and E. N. Jacobsen, Highly Enantioselective, Low-Temperature Epoxidation of Styrene, *J. Am. Chem. Soc.*, 2002, **116**, 9333–9334.
23 H. Yoon and C. J. Burrows, Catalysis of Alkene Oxidation by Nickel Salen Complexes Using Naocl under Phase-Transfer Conditions, *J. Am. Chem. Soc.*, 1988, **110**, 4087–4089.
24 S. Liang and X. R. Bu, Tertiary pentyl groups enhance salen titanium catalyst for highly enantioselective trimethylsilylcyanation of aldehydes, *J. Org. Chem.*, 2002, **67**, 2702–2704.
25 L. E. Martinez, J. L. Leighton, D. H. Carsten and E. N. Jacobsen, Highly Enantioselective Ring-Opening of Epoxides Catalyzed by (Salen)Cr(Iii) Complexes, *J. Am. Chem. Soc.*, 1995, **117**, 5897–5898.
26 J. Meléndez, M. North and R. Pasquale, Synthesis of Cyclic Carbonates from Atmospheric Pressure Carbon Dioxide Using Exceptionally Active Aluminium(salen) Complexes as Catalysts, *Eur. J. Inorg. Chem.*, 2007, **2007**, 3323–3326.
27 M. Taherimehr, A. Decortes, S. M. Al-Amsyar, W. Lueangchaichaweng, C. J. Whiteoak, E. C. Escudero-Adan, A. W. Kleij and P. P. Pescarmona, A highly active Zn (salphen) catalyst for production of organic carbonates in a green CO_2 medium, *Catal. Sci. Technol.*, 2012, **2**, 2231–2237.
28 M. Balas, S. Beaudoin, A. Proust, F. Launay and R. Villanneau, Advantages of Covalent Immobilization of Metal-Salophen on Amino-Functionalized Mesoporous Silica in Terms of Recycling and Catalytic Activity for CO_2 Cycloaddition onto Epoxides, *Eur. J. Inorg. Chem.*, 2021, **2021**, 1581–1591.
29 S. J. Lee, K. L. Mulfort, J. L. O'Donnell, X. Zuo, A. J. Goshe, P. J. Wesson, S. T. Nguyen, J. T. Hupp and D. M. Tiede, Supramolecular porphyrinic prisms: coordinative assembly and solution phase X-ray structural characterization, *Chem. Commun.*, 2006, 4581–4583, DOI: 10.1039/b610025b.
30 F. Song, C. Wang, J. M. Falkowski, L. Ma and W. Lin, Isoreticular chiral metal-organic frameworks for asymmetric alkene epoxidation: tuning catalytic activity by controlling framework catenation and varying open channel sizes, *J. Am. Chem. Soc.*, 2010, **132**, 15390–15398.
31 J. Jiao, C. Tan, Z. Li, Y. Liu, X. Han and Y. Cui, Design and Assembly of Chiral Coordination Cages for Asymmetric Sequential Reactions, *J. Am. Chem. Soc.*, 2018, **140**, 2251–2259.
32 W. Zhou, Q. W. Deng, G. Q. Ren, L. Sun, L. Yang, Y. M. Li, D. Zhai, Y. H. Zhou and W. Q. Deng, Enhanced carbon dioxide conversion at ambient conditions via a pore enrichment effect, *Nat. Commun.*, 2020, **11**, 4481.
33 X. Han, Q. Xia, J. Huang, Y. Liu, C. Tan and Y. Cui, Chiral Covalent Organic Frameworks with High Chemical Stability for Heterogeneous Asymmetric Catalysis, *J. Am. Chem. Soc.*, 2017, **139**, 8693–8697.
34 T. T. Liu, J. Liang, Y. B. Huang and R. Cao, A bifunctional cationic porous organic polymer based on a Salen-(Al) metalloligand for the cycloaddition of carbon dioxide to produce cyclic carbonates, *Chem. Commun.*, 2016, **52**, 13288–13291.
35 J. M. Falkowski, C. Wang, S. Liu and W. Lin, Actuation of asymmetric cyclopropanation catalysts: reversible single-

crystal to single-crystal reduction of metal-organic frameworks, *Angew. Chem., Int. Ed.*, 2011, **50**, 8674–8678.

36 C. F. Zhu, Q. C. Xia, X. Chen, Y. Liu, X. Du and Y. Cui, Chiral Metal-Organic Framework as a Platform for Cooperative Catalysis in Asymmetric Cyanosilylation of Aldehydes, *ACS Catal.*, 2016, **6**, 7590–7596.

37 C. Tan, X. Han, Z. Li, Y. Liu and Y. Cui, Controlled Exchange of Achiral Linkers with Chiral Linkers in Zr-Based UiO-68 Metal-Organic Framework, *J. Am. Chem. Soc.*, 2018, **140**, 16229–16236.

38 T. T. Liu, J. Liang, R. Xu, Y. B. Huang and R. Cao, Salen-Co(iii) insertion in multivariate cationic metal-organic frameworks for the enhanced cycloaddition reaction of carbon dioxide, *Chem. Commun.*, 2019, **55**, 4063–4066.

39 V. Colombo, S. Galli, H. J. Choi, G. D. Han, A. Maspero, G. Palmisano, N. Masciocchi and J. R. Long, High thermal and chemical stability in pyrazolate-bridged metal-organic frameworks with exposed metal sites, *Chem. Sci.*, 2011, **2**, 1311–1319.

40 N. Mosca, R. Vismara, J. A. Fernandes, G. Tuci, C. Di Nicola, K. V. Domasevitch, C. Giacobbe, G. Giambastiani, C. Pettinari, M. Aragones-Anglada, P. Z. Moghadam, D. Fairen-Jimenez, A. Rossin and S. Galli, Nitro-functionalized Bis(pyrazolate) Metal-Organic Frameworks as Carbon Dioxide Capture Materials under Ambient Conditions, *Chem. – Eur. J.*, 2018, **24**, 13170–13180.

41 R. Vismara, G. Tuci, N. Mosca, K. V. Domasevitch, C. Di Nicola, C. Pettinari, G. Giambastiani, S. Galli and A. Rossin, Amino-decorated bis(pyrazolate) metal-organic frameworks for carbon dioxide capture and green conversion into cyclic carbonates, *Inorg. Chem. Front.*, 2019, **6**, 533–545.

42 N. M. Padial, E. Quartapelle Procopio, C. Montoro, E. Lopez, J. E. Oltra, V. Colombo, A. Maspero, N. Masciocchi, S. Galli, I. Senkovska, S. Kaskel, E. Barea and J. A. Navarro, Highly hydrophobic isoreticular porous metal-organic frameworks for the capture of harmful volatile organic compounds, *Angew. Chem., Int. Ed.*, 2013, **52**, 8290–8294.

43 N. Masciocchi, S. Galli, V. Colombo, A. Maspero, G. Palmisano, B. Seyyedi, C. Lamberti and S. Bordiga, Cubic octanuclear Ni(II) clusters in highly porous polypyrazolyl-based materials, *J. Am. Chem. Soc.*, 2010, **132**, 7902–7904.

44 E. Q. Procopio, S. Rojas, N. M. Padial, S. Galli, N. Masciocchi, F. Linares, D. Miguel, J. E. Oltra, J. A. Navarro and E. Barea, Study of the incorporation and release of the non-conventional half-sandwich ruthenium (II) metallodrug RAPTA-C on a robust MOF, *Chem. Commun.*, 2011, **47**, 11751–11753.

45 J. Hu, X. Deng, H. Zhang, Y. Diao, S. Cheng, S. L. Zheng, W. M. Liao, J. He and Z. Xu, Linker Deficiency, Aromatic Ring Fusion, and Electrocatalysis in a Porous Ni8-Pyrazolate Network, *Inorg. Chem.*, 2021, **60**, 161–166.

46 S. Galli, A. Maspero, C. Giacobbe, G. Palmisano, L. Nardo, A. Comotti, I. Bassanetti, P. Sozzani and N. Masciocchi, When long bis(pyrazolates) meet late transition metals: structure, stability and adsorption of metal-organic frameworks featuring large parallel channels, *J. Mater. Chem. A*, 2014, **2**, 12208–12221.

47 T. He, Y. Z. Zhang, B. Wang, X. L. Lv, L. H. Xie and J. R. Li, A Base-Resistant Zn(II) -Based Metal-Organic Framework: Synthesis, Structure, Postsynthetic Modification, and Gas Adsorption, *ChemPlusChem*, 2016, **81**, 864–871.

48 T. He, Z. Huang, S. Yuan, X. L. Lv, X. J. Kong, X. Zou, H. C. Zhou and J. R. Li, Kinetically Controlled Reticular Assembly of a Chemically Stable Mesoporous Ni(II)-Pyrazolate Metal-Organic Framework, *J. Am. Chem. Soc.*, 2020, **142**, 13491–13499.

49 Y.-N. Gong, D.-C. Zhong and T.-B. Lu, Interpenetrating metal–organic frameworks, *CrystEngComm*, 2016, **18**, 2596–2606.

50 R. R. Shaikh, S. Pornpraprom and V. D'Elia, Catalytic Strategies for the Cycloaddition of Pure, Diluted, and Waste CO_2 to Epoxides under Ambient Conditions, *ACS Catal.*, 2017, **8**, 419–450.

51 J. Lan, Y. Qu, Z. Wang, P. Xu and J. Sun, A facile fabrication of a multi-functional and hierarchical Zn-based MOF as an efficient catalyst for CO_2 fixation at room-temperature, *Inorg. Chem. Front.*, 2021, **8**, 3085–3095.

52 M. E. Wilhelm, M. H. Anthofer, M. Cokoja, I. I. E. Markovits, W. A. Herrmann and F. E. Kuhn, Cycloaddition of carbon dioxide and epoxides using pentaerythritol and halides as dual catalyst system, *ChemSusChem*, 2014, **7**, 1357–1360.

53 B.-H. Xu, J.-Q. Wang, J. Sun, Y. Huang, J.-P. Zhang, X.-P. Zhang and S.-J. Zhang, Fixation of CO_2into cyclic carbonates catalyzed by ionic liquids: a multi-scale approach, *Green Chem.*, 2015, **17**, 108–122.

54 Z. Zheng, Z. Wang, Y. Xue, F. He and Y. Li, Selective Conversion of CO_2 into Cyclic Carbonate on Atom Level Catalysts, *ACS Mater. Au*, 2021, **1**, 107–115.

55 L. Hua, B. Li, C. Han, P. Gao, Y. Wang, D. Yuan and Y. Yao, Synthesis of Homo- and Heteronuclear Rare-Earth Metal Complexes Stabilized by Ethanolamine-Bridged Bis(phenolato) Ligands and Their Application in Catalyzing Reactions of CO_2 and Epoxides, *Inorg. Chem.*, 2019, **58**, 8775–8786.

56 Y. T. Zheng, X. Q. Wang, C. Liu, B. Q. Yu, W. L. Li, H. L. Wang, T. T. Sun and J. Z. Jiang, Triptycene-supported bimetallic salen porous organic polymers for high efficiency CO_2 fixation to cyclic carbonates, *Inorg. Chem. Front.*, 2021, **8**, 2880–2888.

57 Y. Z. Li, G. D. Wang, H. Y. Yang, L. Hou, Y. Y. Wang and Z. H. Zhu, Novel cage-like MOF for gas separation, CO_2 conversion and selective adsorption of an organic dye, *Inorg. Chem. Front.*, 2020, **7**, 746–755.

58 C. He, J. Liang, Y.-H. Zou, J.-D. Yi, Y.-B. Huang and R. Cao, Metal-Organic Frameworks Bonded with Metal

N-Heterocyclic Carbenes for efficient catalysis, *Natl. Sci. Rev.*, 2021, DOI: 10.1093/nsr/nwab157.
59 J. Liang, Q. Wu, Y. B. Huang and R. Cao, Reticular frameworks and their derived materials for CO_2 conversion by thermo–catalysis, *EnergyChem*, 2021, **3**, 100064.
60 Y. H. Zou, Y. B. Huang, D. H. Si, Q. Yin, Q. J. Wu, Z. Weng and R. Cao, Porous Metal-Organic Framework Liquids for Enhanced CO_2 Adsorption and Catalytic Conversion, *Angew. Chem., Int. Ed.*, 2021, **60**, 20915–20920.
61 Y. B. N. Tran, P. T. K. Nguyen, Q. T. Luong and K. D. Nguyen, Series of M-MOF-184 (M = Mg, Co, Ni, Zn, Cu, Fe) Metal-Organic Frameworks for Catalysis Cycloaddition of CO_2, *Inorg. Chem.*, 2020, **59**, 16747–16759.